3rd Regional Conference on Noise, Vibration and Comfort (NVC) 2010
28-30th June, 2010, Putrajay, Malaysia
Editors: *M. J. M. Nor, M. Z. Nuawi, A. Arifin, S. M. Haris, N. A. Abdul Jalil and M. Hosseini Fouladi*

THE CONTRIBUTION OF MOMENT EXCITATION ON THE UNCERTAINTY IN THE VIBRATION INPUT POWER TO A STRUCTURE

A. Putra[1] and B. R. Mace[2]
[1]Faculty of Mechanical Engineering
Universiti Teknikal Malaysia Melaka (UTeM)
Melaka, Malaysia
[2]Institute of Sound and Vibration Research (ISVR)
University of Southampton
United Kingdom

ABSTRACT

In structural dynamic systems, there is inevitable uncertainty in the input power from a source to a receiver. Apart from the non-deterministic properties of the vibration source and receiver, there is also uncertainty in the excitation. This comes from the uncertainty of the forcing location on the receiver, its relative phase, its amplitude distribution at multiple contact points and also the spatial separation of these points. Moreover, the uncertainty becomes more significant as only translational force is considered while the moment excitation is often excluded in the calculation. This paper investigates the effect of moment excitation on the uncertainty in the vibration input power to a structure. Quantification of the uncertainty using possibilistic and probabilistic approaches are made. These provide the maximum and minimum bounds and the statistics of the input power, respectively. Expressions for the bounds, mean and variance are presented as well as the frequency band-averaged results.

Keywords: moment excitation; vibration input power; uncertainty; mean; variance.

INTRODUCTION

The treatment of structure-borne sound sources remains a challenging problem. Structural excitation to a building floor, for example, by active components like pumps, compressors, fans and motors is an important mechanism of sound generation. To obtain an accurate prediction of the injected input power from such sources, both the source and the receiver must firstly be characterized (Petersson and Gibbs 2000). However in practical application, the variability of source and receiver properties including the lack of knowledge in the excitation force creates uncertainty in the input power.

Several works have been proposed for source characterization (Petersson and Plunt 1982, Mondot and Petersson 1987) and receiver characterization (Langley and Brown 2004, Langley and Cotoni 2004). With respect to the excitation force, the problem is exacerbated because in practice there will usually be multiple contact points (typically four) and 6 degrees of freedom (3 translation and 3 rotation) at each, and that force and moment components at each contact point will contribute to the total input power. Therefore to assess the uncertainty, some quantification of the bounds, mean and variance of the input power is of interest.

This paper focuses only on the uncertainty in the excitation with the source and receiver assumed to be deterministic. The source may have multiple contact points. Here, the moments are included in the excitation. The uncertainty in input power due to the excitation phase, its location and separation of the contact points is investigated. First some general comments are made. Broadband excitation is described, although only time-harmonic excitation is considered here with frequency averages subsequently being taken. The input power from multiple point forces to an infinite plate is examined to give an insight into the physical mechanisms involved. In practice, the receiver will have modes, although the modal overlap might be high. The input power to a finite plate is then analysed, where now the forcing location at the receiver becomes important. The mean and the variance of the input power averaged over force positions are investigated. The results are also presented in frequency-band averages.

UNCERTAINTY QUANTIFIQATION

Two approaches are employed to describe the uncertainty in the input power, namely possibilistic and probabilistic approaches (Lars 2008). The possibilistic approach gives an interval description of the input power, which lies between lower and upper bounds, i.e.

$$P_{in} \in \left[\underline{P_{in}} \;\; \overline{P_{in}}\right] \tag{1}$$

where $\underline{P_{in}}$ and $\overline{P_{in}}$ are the minimum and maximum bounds and P_{in} is the interval variable. The probabilistic approach gives information about the likelihood and probability of the input power. The variation is specified by a probability density function $\prod$. If $\prod(z)$ is a continuous function of some variable z, the mean μ or the expected value of the input power and its variance σ^2 are defined by

$$\mu_{P_{in}} = \int_z P_{in}(z)\prod(z)dz, \qquad \sigma^2_{P_{in}} = \int_z P^2_{in}(z)\prod(z)dz - \mu^2_{P_{in}} \tag{2}$$

INPUT POWER

Consider a vibrating source connected through a single or N contact points to a

receiver. For a time-harmonic excitation at frequency ω, the input power is expressed as a function of mobility (or impedance) of source and receiver (Cremer *et al.* 2005). This requires knowledge of both source and receiver mobilities and the so-called 'blocked force' or 'free velocity' of the source. In general, the mobilities are matrices and the blocked forces or the free velocities are vectors, with the elements relating to the various translational and rotational degrees of freedoms (DOFs) at the contact points. In this paper, however, the analysis is made by assuming that the force excitation is known and the source mobility is assumed to be much smaller than that of the receiver. The input power is therefore given by

$$P_{in} = \tfrac{1}{2}\Re\left\{\widetilde{\mathbf{F}}^{*}\widetilde{\mathbf{Y}}\widetilde{\mathbf{F}}\right\} \tag{3}$$

where $\widetilde{\mathbf{F}} = [F_1 e^{j\phi_1} \;\; F_2 e^{j\phi_2} \;\; \ldots \;\; F_N e^{j\phi_N}]$ is the vector of the complex amplitude of the time-harmonic forces and where * denotes the conjugate transpose and $\Re$ denotes the real component. The *i*-th force has a real magnitude F_i and phase ϕ_i. The mobilities of the receiver are represented by a $N \times N$ matrix $\widetilde{\mathbf{Y}}$.

Figure 1 illustrates the components of excitation assumed to act on a structure. The response at the contact point is a function of point mobilities, transfer mobilities for different axes and also the cross mobilities for different components. Therefore, there will be a 6×6 mobility matrix for each excitation point. The problem becomes more complicated for multiple contact points. For *N* contact points, the interaction between components will increase the size of the system matrix to $6N \times 6N$.

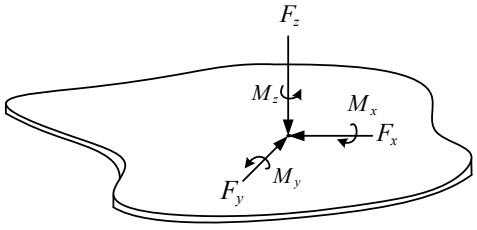

FIGURE 1. Six components of point excitations.

In this paper, however, the problem is simplified by neglecting the in-plane excitations, i.e. F_x, F_y and M_z. Therefore the mobility matrix is reduced to a 3×3 matrix for a single contact point. In general, the input power due to a combined point force and moment excitation can be written as

$$P_{in} = \tfrac{1}{2}\left(\Re\left\{\widetilde{Y}^{vF}\right\}|\widetilde{F}|^2 + 2\Re\left\{\widetilde{Y}^{vM}\right\}\Re\left\{\widetilde{M}\widetilde{F}^{*}\right\} + \Re\left\{\widetilde{Y}^{\dot{\theta}M}\right\}|\widetilde{M}|^2\right) \tag{4}$$

where $\widetilde{Y}^{vF}$ and $\widetilde{Y}^{\dot{\theta}M}$ are the point force and point moment mobilities and $\widetilde{Y}^{vM}$ is the cross-mobilitiy from moment to translation and for an infinite plate

$\Re\{\widetilde{Y}^{vM}\} = 0$. Thus in matrix form, the power can be expressed as in Equation (3) where $\widetilde{\mathbf{F}} = [F_x \; M_x \; M_y]^T$ is the vector of the force and moments. With inclusion of moment excitation, the mobility matrix for a single contact point is given by

$$\widetilde{\mathbf{Y}} = \begin{bmatrix} \widetilde{Y}^{vF} & \widetilde{Y}^{vM_x} & \widetilde{Y}^{vM_y} \\ \widetilde{Y}^{\dot{\theta}_x F} & \widetilde{Y}^{\dot{\theta}_x M_x} & \widetilde{Y}^{\dot{\theta}_x M_y} \\ \widetilde{Y}^{\dot{\theta}_y F} & \widetilde{Y}^{\dot{\theta}_y M_x} & \widetilde{Y}^{\dot{\theta}_y M_y} \end{bmatrix} \tag{5}$$

where $\widetilde{\mathbf{Y}}$ is symmetric.

MAGNITUDE OF MOMENT

The relative contribution to the input power depends of course on the magnitude of the excitation. Force and moment cannot be compared directly as they have different units. In a practical situation, they would also depend on the nature of the force generation mechanism in the source. The installation condition has also to be considered. The effects of moment excitation for a vibrating machine installed on soft support at the contact points would be different to those if the machine were bolted tightly to the receiver structure. Thus the problem remains of qualifying the relative effects of force and moment.

Single contact point

The relative importance of force and moment in exciting a structure can be compared only in terms of their input power. However, to calculate the power, not only the mobilities should be known, but also the magnitudes and the phases of the excitation components (see Equation (4)).

The magnitude of moments, $\widetilde{M} = Me^{j\phi_1}$ and the force, $\widetilde{F} = Fe^{j\phi_2}$ at the contact point are related by an effective lever arm α by

$$M = \alpha F \tag{6}$$

where $0 < \alpha < \infty$. This indicates that if α is very small, the structure is excited mainly by force, while if α is very large the structure is driven mainly by a moment. However, for convenience, a non-dimensional unit is prefered to scale the relative input power. From Equation (4), the total input powers, P_F and P_M, due to a force and a moment are

$$P_{in} = P_F + P_M = \tfrac{1}{2}\Re\{\widetilde{Y}^{vF}\}|\widetilde{F}|^2 + 2\Re\{\widetilde{Y}^{vM}\}\Re\{\widetilde{M}\widetilde{F}^*\} + \tfrac{1}{2}\Re\{\widetilde{Y}^{\dot{\theta}M}\}|\widetilde{M}|^2 \tag{7}$$

For an infinite plate, the real part of the point mobilities are given by

$$\Re\left\{\widetilde{Y}^{vF}\right\}=\frac{\omega}{8Bk^2}, \qquad \Re\left\{\widetilde{Y}^{\dot{\theta}M}\right\}=\frac{\omega}{8B} \tag{8}$$

where ω is the frequency, B is the plate bending stiffness and k is the structural wavenumber. The cross mobility is zero, $\Re\left\{\widetilde{Y}^{vM}\right\}=0$. Consequently, the relative phase between the force and the moment is irrelevant. From Equations (6), (7) and (8), the input power from moment excitation can be scalled in terms of the input power from the force by a non-dimensional unit $k\alpha$ and is expressed as

$$P_M=(k\alpha)^2 P_F \tag{9}$$

Equation (5) can be re-written as

$$P_{in}=\left((k\alpha)^2+1\right)P_F \tag{10}$$

For a finite plate receiver, the total input power is given as in Equation (7) where the phase difference between the force and moment becomes important. While the situation is now numerically complicated, Equation (10) can again be used to scale the individual contribution to the input power.

Multiple contact points

Figure 2 shows a diagram of a translational force F which generates moment M that can be resolved into moments M_x and M_y components. The moments can be expressed as

$$M_x=L\beta F\sin(\delta), \qquad M_y=-L\beta F\cos(\delta) \tag{11}$$

where L is the lever arm, or the distance from the line of action F to the point attached to the structure, δ is the angle between the lever arm and the positive x-axis and β is a dimensionless scaling factor.

Equations (6) and (11) can be used to define the relation between force and moment for multiple contact points. Figure 3 shows the forces and moments for a typical four point contact source, with the points having a rectangular distribution, where $L_3^2=L_1^2+L_2^2$. The reference moment at any contact point might then be considered as a sum of contributions from forces at all the contact points. In this situation, the moment about the x-axis can thus be expressed in the form

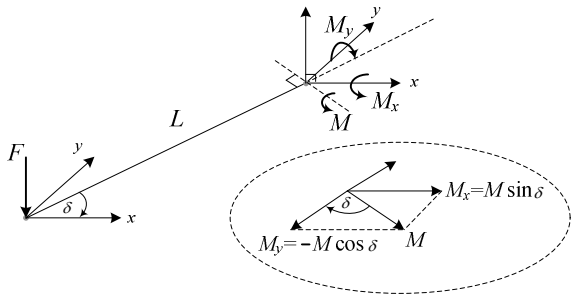

FIGURE 2. The lever arm of the moment and force.

$$\begin{Bmatrix} M_{x,1} \\ M_{x,2} \\ M_{x,3} \\ M_{x,4} \end{Bmatrix} = \begin{bmatrix} \alpha_1 & 0 & -L_2\beta_3 & -L_3\beta_4\sin\theta \\ 0 & \alpha_2 & -L_3\beta_3\sin\theta & -L_2\beta_4 \\ L_2\beta_1 & L_3\beta_2\sin\theta & \alpha_3 & 0 \\ L_3\beta_2\sin\theta & L_2\beta_2 & 0 & \alpha_4 \end{bmatrix} \begin{Bmatrix} F_1 \\ F_2 \\ F_3 \\ F_4 \end{Bmatrix} \tag{12}$$

and the moment about the *y*-axis are

$$\begin{Bmatrix} M_{y,1} \\ M_{y,2} \\ M_{y,3} \\ M_{y,4} \end{Bmatrix} = \begin{bmatrix} \alpha_1 & L_1\beta_2 & 0 & L_3\beta_4\cos\theta \\ L_1\beta_1 & \alpha_2 & -L_3\beta_3\cos\theta & 0 \\ 0 & L_3\beta_2\cos\theta & \alpha_3 & L_1\beta_4 \\ -L_3\beta_1\cos\theta & 0 & -L_1\beta_3 & \alpha_4 \end{bmatrix} \begin{Bmatrix} F_1 \\ F_2 \\ F_3 \\ F_4 \end{Bmatrix} \tag{13}$$

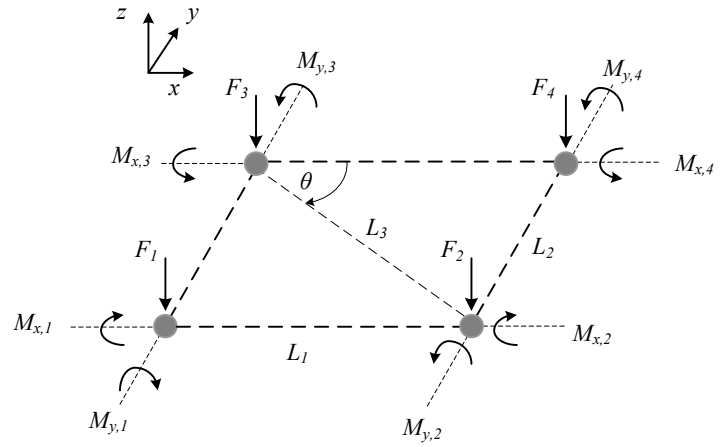

FIGURE 3. The moment and force directions at source-receiver interface with four contact points.

The subsequent sections discuss the results of the effect of moment excitation on the input power to infinite and finite plates particularly for the multiple point excitation. The force and moment mobilities for both infinite and finite plates can be found in (Brennan and Gardonio, 2004).

RESULTS AND DISCUSSION

Single point excitation

Figure 4 shows the normalised total input power (Equation (10)) to an infinite plate for a single contact point. It can be seen that the power from force excitation is constant with frequency while the power from moment excitation is increasing with frequency. Both powers intersect at $k\alpha = 1$. For $k\alpha < 1$, the power is dominated by force excitation and for $k\alpha > 1$, the power is dominated by moment excitation.

Figure 5 shows the normalised input power against $k\alpha$ for a single contact point assuming in-phase force and moment. The plate is an aluminium plate having dimensions $0.65 \times 0.5 \times 0.003$ m. The result in Figure 5(a) shows the increase of the input power due to moment contibution at $k\alpha > 0.25$ (see also Figure 4). For the case where the excitation is near to the plate edge in Figure 5(b), the total power is significantly less at low $k\alpha$, because the point mobility for force excitation (which dominates at low frequencies, $k\alpha << 1$) is smaller near the edge. However, when $k\alpha > 0.2$, the input power is the same as that when the excitation position is near to the centre of the plate due to the increasing power from the moment so that it compensates partly for the reducing power from the force.

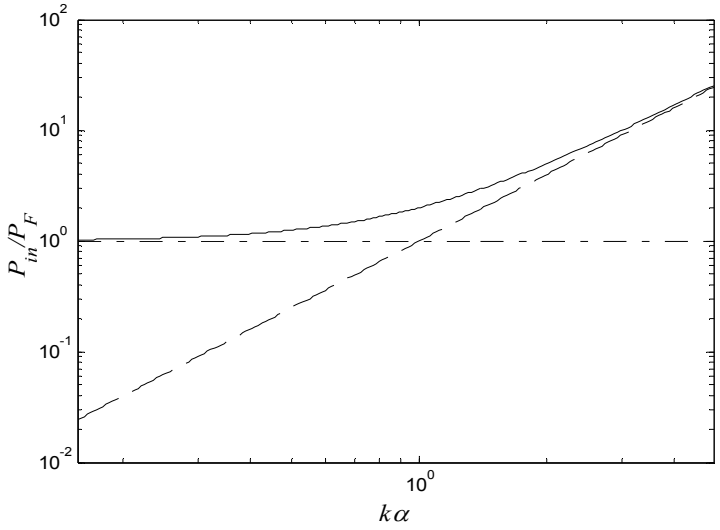

FIGURE 4. The normalised input power from force (– – –) and moment (–) excitations at a single contact point and the total power ( ).

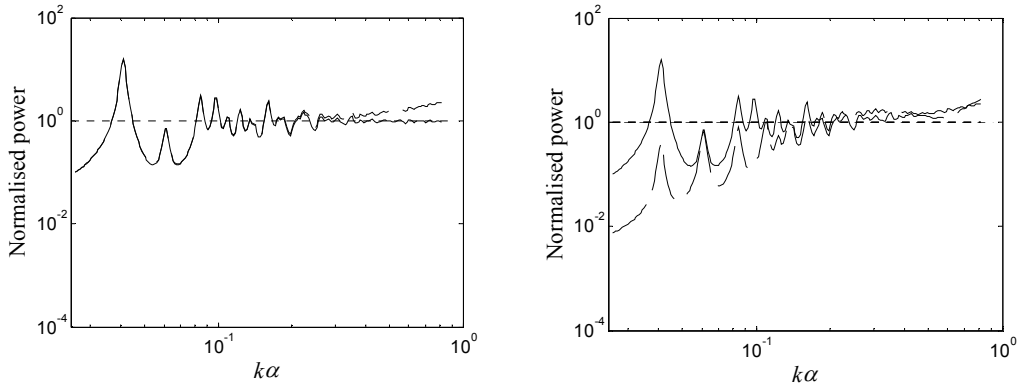

FIGURE 5. The normalised input power of a finite plate subjected to force and moment excitations at a single contact point ((a) the power with (—) and without (– –) moment and (b) the total power for the contact point around the edge (– –) and middle (—) of the plate: $\alpha = 0.005$ m, $\eta = 0.1$).

Figure 6 shows the normalised input power for various forcing locations on the plate. The increase in the mean power due to the contribution of moment excitation can be seen roughly above $k\alpha = 0.35$.

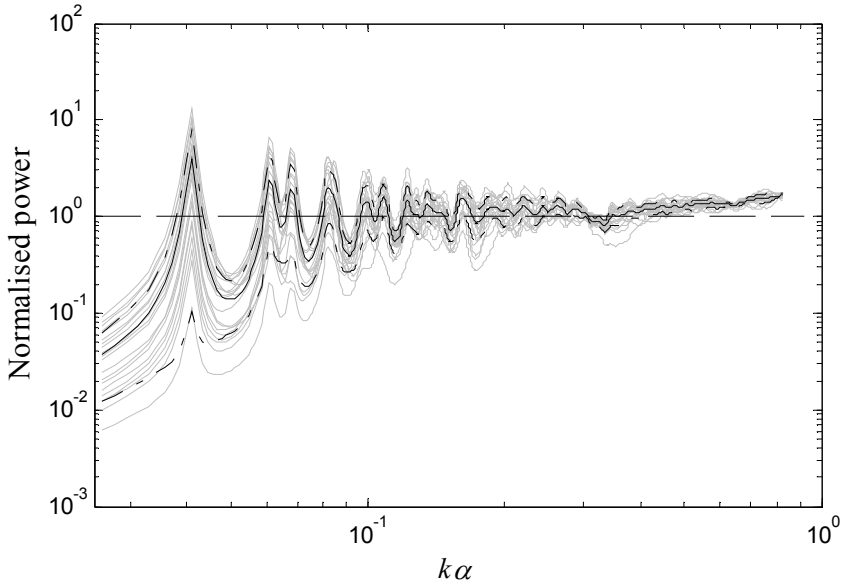

FIGURE 6. The normalised input power (light dark) of a finite plate subjected to force and moment excitations at single contact point for various possible forcing locations: —— mean and , – · – mean±standard ($\eta = 0.1$, $\alpha = 0.005$ m).

Multiple point excitations

As an example, for two contact points there are fifteen relative phases. Assume the distance L between the two points is parallel with x-axis ($\delta = 0$) so that some transfer moment mobilities about x-axis become zero. The transfer moment mobilities are given in Appendix. In this case, the total input power for the case of two contact points is given by

$$\begin{aligned} P_{in} = {} & \tfrac{1}{2}\Re\left\{\widetilde{Y}_p^{\,vF}\right\}(F_1^2 + F_2^2) + \tfrac{1}{2}\Re\left\{\widetilde{Y}_p^{\,\dot{\theta}_x M_x}\right\}(M_{x,1}^2 + M_{x,2}^2) + \tfrac{1}{2}\Re\left\{\widetilde{Y}_p^{\,\dot{\theta}_y M_y}\right\}(M_{y,1}^2 + M_{y,2}^2) + \\ & \Re\left\{\widetilde{Y}_t^{\,vF}\right\}F_1 F_2 \cos\varphi_1 + \Re\left\{\widetilde{Y}_t^{\,\dot{\theta}_x M_x}\right\}M_{x,1}M_{x,2}\cos\varphi_2 + \Re\left\{\widetilde{Y}_t^{\,\dot{\theta}_y M_y}\right\}M_{y,1}M_{y,2}\cos\varphi_3 + \\ & \Re\left\{\widetilde{Y}_t^{\,vM_y}\right\}(F_2 M_{y,1}\cos\varphi_4 + F_1 M_{y,2}\cos\varphi_5) \end{aligned} \tag{14}$$

where Y_p denotes the point mobility (the same contact point) and Y_t denotes the transfer mobility (different contact point). The phase φ denotes the relative phase between the two components at the same or different contact points, for example φ_4 is the relative phase between the moment about the y-axis and the force at different points. In Equation (14), it has been noted that $\widetilde{Y}_t^{\,vM_y} = \widetilde{Y}_t^{\,\dot{\theta}_y F}$. Due to the complexity of this expression, it is difficult to determine the bounds of input power analytically. However for simplicity, if it is assumed that all the components are in-phase, so that $\varphi_i = 0$ for $i = 1,2,3,4,5$. By also assuming $F_1 = F_2 = F$, $\alpha_1 = \alpha_2$ and following the same method as in Equations (12) and (13) for 2×2 matrix, thus $M_{x,1} = M_{x,2} = \alpha F$ and $M_{y,1} = (\alpha + \beta L)F$ and $M_{y,1} = (\alpha - \beta L)F$. The asymptotic forms of the transfer mobility in Equation (14) for this case can be expressed as

$$\widetilde{Y}_t^{\,vM_y} = \frac{2}{k}\Re\left\{\widetilde{Y}_p^{\,\dot{\theta}_y M_y}\right\}\sqrt{\frac{2}{\pi kL}}\left(\sin(kL - \pi/4) - j\sin(kL - 3\pi/4)\right) \tag{15a}$$

$$\Re\left\{\widetilde{Y}_t^{\,\dot{\theta}_x M_x}\right\} = \frac{2}{kL}\Re\left\{\widetilde{Y}_p^{\,\dot{\theta}_x M_x}\right\}\sqrt{\frac{2}{\pi kL}}\sin(kL - \pi/4) \tag{15b}$$

$$\Re\left\{\widetilde{Y}_t^{\,\dot{\theta}_y M_y}\right\} = 2\Re\left\{\widetilde{Y}_p^{\,\dot{\theta}_y M_y}\right\}\sqrt{\frac{2}{\pi kL}}\left(\cos(kL - \pi/4) - \frac{1}{kL}\sin(kL - 3\pi/4)\right) \tag{15c}$$

By substituting Equation (15) into Equation (14) and setting the cos and sin terms equal to unity, the maximum and minimum bounds of the input power normalised with respect to the input power from translational force (P_F) for in-phase excitation are found to be

$$\frac{\overline{P_{in}}}{2P_F} = 1 + (k\alpha)^2 + \frac{(k\beta L)^2}{2} \pm \sqrt{\frac{2}{\pi kL}}\left[1 + (k\alpha)^2 - (k\beta L)^2 + \frac{(k\beta L)^2}{kL}\right] \tag{16}$$

For the case when $k\alpha << 1$ and $k\beta L << 1$, Equation (16) reduces to

$$\frac{\overline{P_{in}}}{2P_F} = 1 \pm \sqrt{\frac{2}{\pi kL}} \tag{17}$$

i.e. where the moment excitation is neglected (see again Figure (4)).

Assuming random phases with equal probability in Equation (14), the mean and the variance of the input power to an infinite plate receiver through N contact points can, in general, be expressed as

$$\mu_{P_{in}} = \tfrac{1}{2}\sum_{i}^{N}\left(\Re\left\{\tilde{Y}_{ii}^{\,vF}\right\}F_i^2 + \Re\left\{\tilde{Y}_{ii}^{\,\dot{\theta}_{x,y}M_{x,y}}\right\}M_{x,y(i)}^2\right) \tag{18}$$

$$\begin{aligned}\sigma_{P_{in}}^2 = {} & \tfrac{1}{2}\sum_{i=1}^{N-1}\sum_{\substack{k=2\\k>i}}^{N}\left(\Re\left\{\tilde{Y}_{ik}^{\,vF}\right\}F_iF_k\right)^2 + \tfrac{1}{2}\sum_{i=1}^{N-1}\sum_{\substack{k=2\\k>i}}^{N}\left(\Re\left\{\tilde{Y}_{ik}^{\,\dot{\theta}_{x,y}M_{x,y}}\right\}M_{x,y(i)}M_{x,y(k)}\right)^2 \\ & + \tfrac{1}{2}\sum_{i=1}^{N-1}\sum_{\substack{k=2\\k>i}}^{N}\left(\Re\left\{\tilde{Y}_{ik}^{\,\dot{\theta}_{x,y}F}\right\}F_iM_{x,y(k)}\right)^2 + \tfrac{1}{2}\sum_{i=1}^{N-1}\sum_{\substack{k=2\\k>i}}^{N}\left(\Re\left\{\tilde{Y}_{ik}^{\,vM_{x,y}}\right\}M_{x,y(i)}F_k\right)^2\end{aligned} \tag{19}$$

where i and k indicate the i-th and k-th contact points, respectively.

The bounds of the normalised standard deviation can be obtained by substituting Equation (15) into Equation (19). After algebraic manipulation, it can be approximated by

$$\frac{\overline{\sigma}}{2P_F} \approx \sqrt{\frac{2}{\pi kL}}\left[1 + \frac{(k\alpha)^4}{(kL)^2} + ((k\alpha)^2 - (k\beta L)^2)^2 + 2((k\alpha)^2 + (k\beta L)^2)\right]^{1/2} \tag{20}$$

Again, for $k\alpha << 1$ and $k\beta L << 1$, this yields the standard deviation for force excitation

$$\frac{\overline{\sigma}}{2P_F} \approx \sqrt{\frac{2}{\pi kL}} \tag{22}$$

Figure 6 shows the mean input power and its standard deviation for an infinite plate with two contact points. It can be seen that the input power tends to increase at high frequencies due to contribution of the moment excitations.

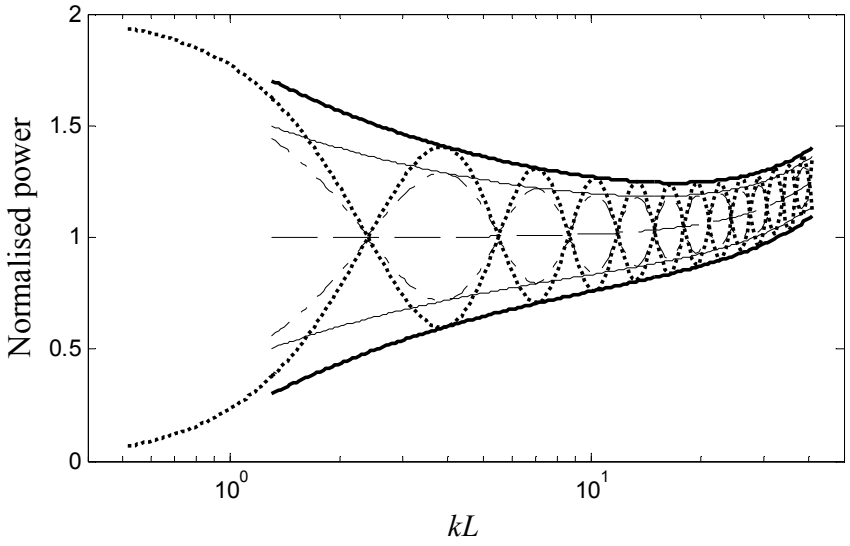

FIGURE 5. The normalised input power of a finite plate subjected to two harmonic unit point forces and two harmonic moments: – – mean, — (thick line) max/min bounds; Equation (14), – · – mean±standard deviation, — mean±bounds of standard deviation; Equation (18) ($\alpha = 0.003$ m, $\beta = 0.003, \eta = 0.1$).

Again for a finite plate, the relative phases due to coupling between forces and moments are of interest for multiple contact points. The mean power, assuming the relative phases between the excitations are equally probable, i.e. the same as that in Equation (18) for an infinite plate. However, a force will produce a rotation and a moment will produce a displacement at the same point. Therefore the variance is given by

$$\begin{aligned}\sigma^2_{P_{in}} = &\tfrac{1}{2}\sum_{i=1}^{N-1}\sum_{\substack{k=2\\k>i}}^{N}\left(\Re\left\{\widetilde{Y}_{ik}^{\,vF}\right\}F_iF_k\right)^2+\tfrac{1}{2}\sum_{i=1}^{N-1}\sum_{\substack{k=2\\k>i}}^{N}\left(\Re\left\{\widetilde{Y}_{ik}^{\,\dot\theta_{x,y}M_{x,y}}\right\}M_{x,y(i)}M_{x,y(k)}\right)^2\\ &+\tfrac{1}{2}\sum_{i=1}^{N-1}\sum_{\substack{k=1\\k\geq i}}^{N}\left(\Re\left\{\widetilde{Y}_{ik}^{\,\dot\theta_{x,y}F}\right\}F_iM_{x,y(k)}\right)^2+\tfrac{1}{2}\sum_{i=1}^{N-1}\sum_{\substack{k=1\\k\geq i}}^{N}\left(\Re\left\{\widetilde{Y}_{ik}^{\,vM_{x,y}}\right\}M_{x,y(i)}F_k\right)^2\end{aligned} \tag{22}$$

For four contact points, the mobility matrices are 12×12 times. Using Equations (18) and (22), Figure 6 shows the mean and standard deviation of the input power for damping loss factor $\eta = 0.05$. The spatial separation of the contact points is again assumed to form a rectangular shape and L is the length of the diagonal. The results agree well with those from the infinite plate above $kL = 10$. Below this, the agreement deteriorates due to small damping. This is clearly shown in

the relative standard deviation, $r_\sigma = \sigma / \mu$, plotted in Figure 7. However, it can be seen that the numerical result has a good agreement with that from the relative standard deviation from the mean and standard deviation of the input power of a rectangular plate subjected to a point force averaged over all possible forcing locations and frequency bands given by

$$r_\sigma = \frac{1}{\sqrt{\pi n_d \eta \omega}} \tag{23}$$

where n_d is the modal density of the plate.

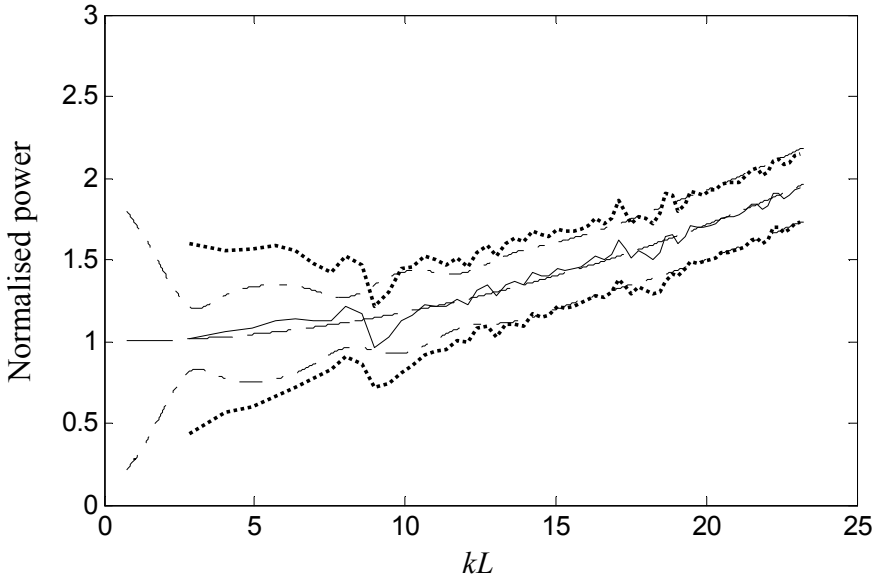

FIGURE 6. The normalised input power of a finite plate subjected to force and moment excitation at four contact points averaged over various possible forcing locations and frequency bands: mean (—— numerical calculation, – – infinite plate) and mean±standard deviation (···· numerical calculation, – · – infinite plate) ($L = 0.14$ m, $\eta = 0.05$, $\alpha = 0.005$ m, $\beta = 0.005$).

CONCLUSIONS

The relative effect of moment excitation can be expressed in terms of a force and a distance corresponding to a characteristic of the source. It can also be scalled as a function of the input power of the force and the structural wavenumber. This effect tends to increase as frequency increases. The expressions for the bounds, mean and variance of the input power have also been presented. The contribution to the total input power can be predicted using the simple expression of the relative standard deviation for the force.

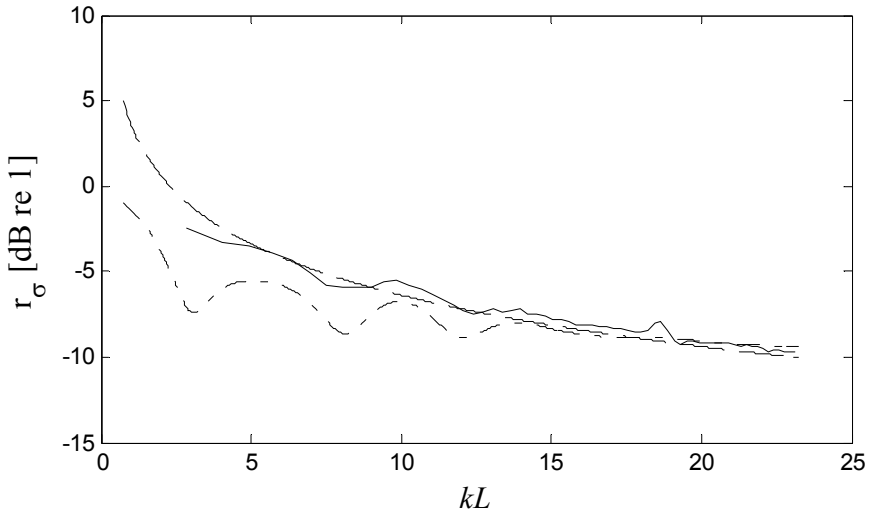

FIGURE 7. The relative standard deviation of the input power:
— numerical calculation, – · – infinite plate, – – Equation (23)

ACKNOWLEDGEMENTS

The authors gratefully acknowledge the financial support provided by The Engineering and Physical Sciences Research Council (EPSRC), United Kingdom under grant EP/D002 15X/1.

REFERENCES

Brennan, M. J. and Gardonio, P. Mobility and impedance methods in structural dynamics. Chapter 9 in *Advanced Applications in Acoustics, Noise and Vibration* (Eds. F. J. Fahy and J. G. Walker). Spon Press, 2004.

Cremer, L., Heckl, M. & Petersson, B. A. T. 2005. *Structure Borne Sound*, Springer, Berlin, 3rd Ed.

Hinke, L. 2008. Modelling approaches for the low-frequency analysis of the built-up structures with non-deterministic properties, Ph.D thesis, University of Southampton, 2008.

Langley, R. S. & Brown, A. W. M. 2004. The ensemble statistics of the energy of a random system subjected to harmonic excitation, *Journal of Sound and Vibration*, 275, pp. 823-846.

Langley, R. S. & Brown, A. W. M. 2004. The ensemble statistics of the band-averaged energy of a random system, *Journal of Sound and Vibration*, 275, pp. 847-857.

Langley, R. S. & Cotoni, V. 2004. Response variance prediction in the statistical energy analysis of built-up systems, *Journal of Acoustical Society of America*, 115, pp. 706-718.

Mondot, J. M. & Petersson, B. A. T. 1987. Characterization of structure-borne sound sources: the source descriptor and coupling function, *Journal of Sound and Vibration*, 114, pp. 507-518.

Petersson, B. A. T. & Gibbs, B. M. 2000. Towards a structure-borne sound source characterisation, *Applied Acoustics*, 61, pp. 325-343.

Petersson, B. A. T. & Plunt, J. 1982. On effective mobilities in the prediction of structure-borne sound transmission between a source structure and a receiving structure. Part I: Theoretical background and basic experimental studies, *Journal of Sound and Vibration*, 82, pp. 517-529.

Petersson, B. A. T. & Plunt, J. 1982. On effective mobilities in the prediction of structure-borne sound transmission between a source structure and a receiving structure. Part II: Procedures for the estimation of mobilities, *Journal of Sound and Vibration*, 82, 531--540.